


Carbon-Based Perovskite Solar Cell †

Luigi Vesce ^{1,*}, Maurizio Stefanelli ² and Aldo Di Carlo ^{1,2}

¹ Centre for Hybrid and Organic Solar Energy (CHOSE), Department of Electronic Engineering, University of Rome “Tor Vergata”, Via del Politecnico 1, 00133 Roma, Italy; aldo.dicarlo@uniroma2.it

² Istituto di Struttura della Materia, Consiglio Nazionale delle Ricerche (ISM-CNR), Via del Fosso del Cavaliere 100, 00133 Roma, Italy; maurizio.stefanelli@uniroma2.it

* Correspondence: vesce@ing.uniroma2.it

† Presented at the 4th International Online Conference on Nanomaterials, 5–19 May 2023; Available online: <https://iocn2023.sciforum.net/>.

Abstract: In a short period, Perovskite solar cell (PSC) technology gained high efficiency and broad attention because of its key enabling physical and morphological features. One of the main obstacles to the PSC industrialization and commercialization deals with the demonstration of stable devices by adopting low-cost and reliable materials and fabrication methods. In the n-i-p structure, the organic hole-transporting layer and the metal counter-electrodes are the main causes of instability and high cost. Here, we substituted these two elements with a low-temperature and low-cost carbon-based counter electrode.

Keywords: perovskite solar cell; carbon; nanomaterial; low cost; hole transporting layer; stability; printing technique

1. Introduction

The constant and unceasing progress of technology in different areas requires renewable and green energy sources [1]. The photovoltaic (PV) sector has a fundamental role to cover the energy demand. To date, the PV market has been based mainly on the “first-generation” technology, i.e., monocrystalline and polycrystalline silicon, because of its high conversion efficiency of solar radiation into electricity. Despite that, the expensive manufacturing processes of silicon and its decreasing availability in nature have accelerated the exploitation of “second-generation” thin-film technologies based on materials such as cadmium telluride (CdTe) and amorphous silicon (a-Si) [2]. Moreover, the “third-generation” PV aims to maintain high efficiency by reducing production costs thanks to hybrid-organic materials on rigid and flexible substrates [3–6]. Natural dyes such as anthocyanins [7], polymers [8] and fullerenes [9] are just a few examples of molecules used for this purpose. The main issue concerning these new technologies is stability, since the organic molecules used are very sensitive to the operating conditions, such as temperature, prolonged exposure to UV light and humidity. The toxicity of the materials used and the synthesis/purification costs are issues to be addressed.

In the recent years, Perovskite (PVSK) has been widely used as photo-generator [10–12]. Its optical and electronic properties have allowed continuous development, reaching record efficiencies (close to 26%) in a few years [13]. PVSK is a chemical compound with an ABX_3 formula, where A and B are cations with different atomic radii, and X represents an anion. Currently, regarding PVSKs, we refer to all crystalline solids with the same structure as $CaTiO_3$ (bipyramidal crystalline cell with square base). Recently, perovskite-based materials—organometallic compounds of halogens—have gathered particular interest in the PV field thanks to their easy processability by solution together with efficiency comparable to the best inorganic materials used in optoelectronics such as gallium arsenide (GaAs) and Si.



Citation: Vesce, L.; Stefanelli, M.; Di Carlo, A. Carbon-Based Perovskite Solar Cell. *Mater. Proc.* **2023**, *14*, 29. <https://doi.org/10.3390/IOC2023-14539>

Academic Editor: Minas Stylianakis

Published: 5 May 2023



Copyright: © 2023 by the authors. Licensee MDPI, Basel, Switzerland. This article is an open access article distributed under the terms and conditions of the Creative Commons Attribution (CC BY) license (<https://creativecommons.org/licenses/by/4.0/>).

Typically, a PVS solar cell (PSC) is a layered structure, where each layer performs a well-defined function affecting the performance and the stability of the device. The PVS is sandwiched between one electron transport layer (ETL) and a hole transport layer (HTL). The ETL and HTL are both connected to an external circuit by gold or silver contacts. In case of n-i-p architecture, ETL is generally composed by c-TiO₂ (compact TiO₂) and mp-TiO₂ (mesoporous TiO₂) or SnO₂ and guarantees good conduction, low charge recombination and high transparency. The most widespread HTL is the 2,2',7,7'-Tetrakis(N,N-di-p-methoxyphenylamine)-9,9'-spirobifluorene. Spiro-MeOTAD ensures good energy levels of the band gap, a quick charge transfer and low recombination. However, there are still many related problems concerning the use of this material, e.g., operational environment sensitivity, high cost (about EUR 200/g), complex synthesis and low yield [14]. Moreover, spiro-OMeTAD is doped to increase the mobility of the holes with highly hygroscopic salts (lithiumbis(trifluoromethylsulfonyl)imide (Li-TFSI) or 4-tert-butylpyridine (t-BP)), leading to PSC degradation deterioration. Regarding the metal counter-electrode, gold diffuses into the structure of the device when exposed to continuous lighting, which causes damage. It is possible to replace both the organic HTL and the metal electrode with one low-temperature conductive carbon layer. Carbon materials are cheap when compared to HTMs (hole-transporting materials) and gold, resulting in a reduction of cells cost and an increase in stability. Carbon is a key material widely used in the PV field due to its abundance, low cost and appropriate energy level. Different kind of carbon materials [15–17], such as carbon nanotubes, carbon fiber and graphene, have been applied with success in many PV devices. In the PVS field, the efficiencies are competitive with those measured in devices using spiro-OMeTAD as HTM [18–23]. Low-temperature carbon pastes, unlike the porous high-temperature inks [17,21], can be processed at temperatures below 130 °C, exhibiting features of high conductivity, low cost, good stability and high throughput processes.

In this paper, we demonstrate a simple process to fabricate HTL- and gold-free PSCs based on low-temperature carbon counter-electrodes by adopting solution-based processes for the full cell stack.

2. Materials and Methods

We adopted large area (1.01 cm²) of n-i-p cells as reported in Figure 1a.

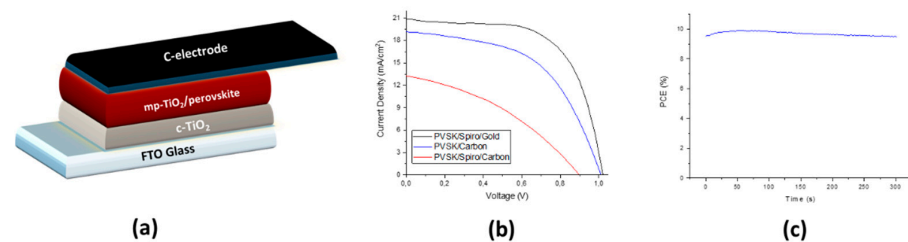


Figure 1. (a) PSC layers; (b) JV curves measurements; (c) Stability by MPP tracking.

We cleaned the FTO (fluorinated tin oxide) glasses (NSG, 8 Ω/sq.) in an ultrasonic system using subsequent solvents (soap/water, acetone, ethanol and isopropanol) for 5 min each. We deposited 30 nm-thick c-TiO₂ as reported in [24] and 250 nm-thick mp-TiO₂ paste (Great Cell Solar 18 nrt, diluted with ethanol 1:4 *w/w*) by the spin-coating, method followed by 30 min @ 500 °C sintering in an oven. The substrates were exposed to an UV lamp, and then we deposited the triple cation PVS (Cs_{0.05}(MA_{0.17}FA_{0.83})_{0.95}Pb(I_{0.83}Br_{0.17})₃ in DMF/DMSO, 1.42 M) (PbI₂ from TCI Co., Ltd., Tokyo, Japan; CsI, FAI and MABr from Great Cell Solar, Queanbeyan, Australia) by the spin-coating method in a glovebox. The spin-coating parameters to deposit the precursor solution were as follows: first step: 1000 rpm, 5 s ramping, 10 s; second step: 5000 rpm, 2 s ramping, 30 s; chlorobenzene dropped 7 s before the end. Then, the PVS was annealed 60 min @ 100 °C. In a recent publication, we demonstrated how to upscale the triple cation PVS formulation to the module device [24]. Regarding the gold-based cells, a Spiro-OMeTAD (Borum, Hadsten, Denmark)

HTM solution was prepared and deposited according to [14]. Following this, 85 nm-thick gold and 30 μm carbon (Dyename, Stockholm, Sweden) counter-electrodes were thermally evaporated and blade-coated, respectively. The carbon-based cells were annealed at 60 °C in vacuum and 120 °C in air for 15 min in the case of Spiro HTM and HTM-free, respectively. The JV curves and the stability measurements were reported by a Keithley source meter/LabVIEW under a class A sun simulator (Sun 2000, Abet, Milford, Connecticut, USA) at AM 1.5 1000 W/m² calibrated by a Skye Instruments sensor Ltd (Llandrindod Wells, UK).

3. Results and Discussion

The JV curves are depicted in Figure 1b and Table 1.

Table 1. Electrical parameters of the fabricated devices. HI is the Hysteresis Index [25].

Cell Stack	Voc (V)	J _{sc} (mA/cm ²)	FF (%)	PCE (%)	HI
TiO ₂ /PVSK/Spiro/Carbon	0.90	12.67	39	4.40	1.20
TiO ₂ /PVSK/Carbon	1.01	19	53	10.20	1.05
TiO ₂ /PVSK/Spiro/Gold	1.02	20.30	65	13.40	1.25

In the case of PVSK/Spiro/carbon cells, all electrical parameters were lower with respect to the PVSK/carbon cells. Most likely, capacitive and recombination phenomena occurred at the Spiro/Carbon interface, with this inefficient setup affecting not only the fill factor, but also the current and Voc. A lower FF mainly affected the PCE, as shown by the comparison of PVSK/carbon with PVSK/HTL/Gold cells, due to the lower conductivity of the carbon electrode compared to the gold electrode. It is also important to underline how the hysteresis phenomena are practically absent in the case of carbon-based cells by comparing the hysteresis index (HI) in Table 1 [26]. In the case of PVSK/carbon cells, the short-circuit current density (J_{sc}) was about 19 mA/cm², as reported in Figure 1b and Table 1. The best efficiencies were 13.4% and 10.2% for the PVSK/HTL/Gold and PVSK/Carbon devices, respectively (Figure 1b, Table 1). After 5 min in the light condition at maximum power, the device lost just 4% efficiency and remained stable at 9.8% (Figure 1c, Table 1).

4. Conclusions

The PV exploitation should avoid high-cost and high-CO₂ footprint materials and fabrication processes. The adoption of low-temperature carbon PSC counter-electrodes makes it possible to avoid expensive organic HTM and metal counter-electrodes, such as gold and silver. These materials are also sources of degradation, leading to low stability in the presence of moisture, high temperature and light. Moreover, the carbon inks can be deposited by large-area printing techniques, such as screen-printing and blade-coating [27]. Since the carbon layer can be annealed at temperatures less than 120 °C, the impact from the LCA (life cycle assessment) point of view is low. Here, we demonstrated how the PSCs can work without any HTL or loss of efficiency. Further, studies on low-cost 2D PVSK strategies are ongoing to improve the electrical parameters of the cells. Moreover, the scaling up to module and stability assessment according to the ISOS standard is ongoing.

Author Contributions: Conceptualization, L.V.; methodology, L.V.; validation, L.V. and A.D.C.; formal analysis, L.V. and M.S.; investigation, M.S. and L.V.; resources, A.D.C.; data curation, L.V. and M.S.; writing—original draft preparation, L.V.; writing—review and editing, L.V.; visualization, L.V.; supervision, A.D.C. and L.V.; project administration, A.D.C. and L.V.; funding acquisition, A.D.C. and L.V. All authors have read and agreed to the published version of the manuscript.

Funding: This research was funded by the European Union's Horizon 2020 programme, through an FET Proactive research and innovation action under grant agreement No. 101084124 (DIAMOND). The authors acknowledge the project UNIQUE, supported under the umbrella of SOLARERA. NET_cofund by ANR, P_{tj}, MUR (GA 775970), MINECOAEI, SWEA, within the European Union Framework Program for Research and Innovation Horizon 2020 (Cofund ERANET Action, No. 691664).

Institutional Review Board Statement: Not applicable.

Informed Consent Statement: Not applicable.

Data Availability Statement: Data supporting reported results are available in repository.

Conflicts of Interest: The authors declare no conflict of interest.

References

1. Eftekharijad, S.; Vittal, V.; Heydt, G.T.; Keel, B.; Loehr, J. Impact of increased penetration of photovoltaic generation on power systems. *IEEE Trans. Power Syst.* **2013**, *28*, 893–901. [[CrossRef](#)]
2. Barkhouse, D.A.R.; Gunawan, O.; Gokmen, T.; Todorov, T.K.; Mitzi, D.B. Yield predictions for photovoltaic power plants: empirical validation, recent advances and remaining uncertainties. *Prog. Photovolt. Res. Appl.* **2015**, *20*, 6–11. [[CrossRef](#)]
3. Mincuzzi, G.; Vesce, L.; Liberatore, M.; Reale, A.; Di Carlo, A.; Brown, T.M. Laser-sintered TiO₂ films for dye solar cell fabrication: An electrical, morphological, and electron lifetime investigation. *IEEE Trans. Electron Devices* **2011**, *58*, 3179–3188. [[CrossRef](#)]
4. Barichello, J.; Vesce, L.; Mariani, P.; Leonardi, E.; Braglia, R.; Di Carlo, A.; Canini, A.; Reale, A. Stable semi-transparent dye-sensitized solar modules and panels for greenhouse application. *Energies* **2021**, *14*, 6393. [[CrossRef](#)]
5. Zardetto, V.; De Angelis, G.; Vesce, L.; Caratto, V.; Mazzuca, C.; Gasiorowski, J.; Reale, A.; Di Carlo, A.; Brown, T.M. Formulations and processing of nanocrystalline TiO₂ films for the different requirements of plastic, metal and glass dye solar cell applications. *Nanotechnology* **2013**, *24*, 255401. [[CrossRef](#)]
6. Dominici, L.; Vesce, L.; Colonna, D.; Michelotti, F.; Brown, T.M.; Reale, A.; Di Carlo, A. Angular and prism coupling refractive enhancement in dye solar cells. *Appl. Phys. Lett.* **2010**, *96*, 42. [[CrossRef](#)]
7. Yuvapragasam, A.; Muthukumarasamy, N.; Agilan, S.; Velauthapillai, D.; Senthil, T.S.; Sundaram, S. Natural dye sensitized TiO₂ nanorods assembly of broccoli shape based solar cells. *J. Photochem. Photobiol. B Biol.* **2015**, *148*, 223–231. [[CrossRef](#)]
8. Etxebarria, I.; Ajuria, J.; Pacios, R. Solution-processable polymeric solar cells: A review on materials, strategies and cell architectures to overcome 10%. *Org. Electron.* **2015**, *19*, 34–60. [[CrossRef](#)]
9. Zhang, G.; Ning, H.; Chen, H.; Jiang, Q.; Jiang, J.; Han, P.; Dang, L.; Xu, M.; Shao, M.; He, F.; et al. Naphthalenothiophene imide-based polymer exhibiting over 17% efficiency. *Joule* **2021**, *5*, 931–944. [[CrossRef](#)]
10. Kojima, A.; Teshima, K.; Shirai, Y.; Miyasaka, T. Organometal halide perovskites as visible-light sensitizers for photovoltaic cells. *J. Am. Chem. Soc.* **2009**, *131*, 6050–6051. [[CrossRef](#)]
11. Snaith, H.J. Present status and future prospects of perovskite photovoltaics. *Nat. Mater.* **2018**, *17*, 372–376. [[CrossRef](#)] [[PubMed](#)]
12. Feng, S.-P.; Cheng, Y.; Yip, H.-L.; Zhong, Y.; Fong, P.W.K.; Li, G.; Ng, A.; Chen, C.; Castriotta, L.A.; Matteocci, F.; et al. Roadmap on Commercialization of Metal Halide Perovskite Photovoltaics. *J. Phys. Mater.* **2023**, *6*, 032501. [[CrossRef](#)]
13. Green, M.A.; Dunlop, E.D.; Hohl-Ebinger, J.; Yoshita, M.; Kopidakis, N.; Bothe, K.; Hinken, D.; Rauer, M.; Hao, X. Solar cell efficiency tables (Version 60). *Prog. Photovolt. Res. Appl.* **2022**, *30*, 687–701. [[CrossRef](#)]
14. Vesce, L.; Stefanelli, M.; Di Carlo, A. Efficient and stable perovskite large area cells by low-cost fluorene-xantene-based hole transporting layer. *Energies* **2021**, *14*, 6081. [[CrossRef](#)]
15. Calabrò, E.; Matteocci, F.; Paci, B.; Cinà, L.; Vesce, L.; Barichello, J.; Generosi, A.; Reale, A.; Di Carlo, A. Easy Strategy to Enhance Thermal Stability of Planar PSCs by Perovskite Defect Passivation and Low-Temperature Carbon-Based Electrode. *ACS Appl. Mater. Interfaces* **2020**, *12*, 32536–32547. [[CrossRef](#)]
16. Barichello, J.; Vesce, L.; Matteocci, F.; Lamanna, E.; Di Carlo, A. The effect of water in Carbon-Perovskite Solar Cells with optimized alumina spacer. *Sol. Energy Mater. Sol. Cells* **2019**, *197*, 76–83. [[CrossRef](#)]
17. Vesce, L.; Riccitelli, R.; Mincuzzi, G.; Orabona, A.; Soscia, G.; Brown, T.M.; Di Carlo, A.; Reale, A. Fabrication of spacer and catalytic layers in monolithic dye-sensitized solar cells. *IEEE J. Photovolt.* **2013**, *3*, 1004–1011. [[CrossRef](#)]
18. Stefanelli, M.; Vesce, L.; Di Carlo, A. Upscaling of Carbon-Based Perovskite Solar Module. *Nanomaterials* **2023**, *13*, 313. [[CrossRef](#)]
19. Liu, Z.; Shi, T.; Tang, Z.; Sun, B.; Liao, G. Using a low-temperature carbon electrode for preparing hole-conductor-free perovskite heterojunction solar cells under high relative humidity. *Nanoscale* **2016**, *8*, 7017–7023. [[CrossRef](#)]
20. Chu, Q.Q.; Ding, B.; Qiu, Q.; Liu, Y.; Li, C.X.; Li, C.J.; Yang, G.J.; Fang, B. Cost effective perovskite solar cells with a high efficiency and open-circuit voltage based on a perovskite-friendly carbon electrode. *J. Mater. Chem. A* **2018**, *6*, 8271–8279. [[CrossRef](#)]
21. Bogachuk, D.; Zouhair, S.; Wojciechowski, K.; Yang, B.; Babu, V.; Wagner, L.; Xu, B.; Lim, J.; Mastroianni, S.; Pettersson, H.; et al. Low-Temperature Carbon-based Electrodes in Perovskite Solar Cells. *Energy Environ. Sci.* **2020**, *13*, 3880–3916. [[CrossRef](#)]
22. Jiang, P.; Jones, T.W.; Duffy, N.W.; Anderson, K.F.; Bennett, R.; Grigore, M.; Marvig, P.; Xiong, Y.; Liu, T.; Sheng, Y.; et al. Fully printable perovskite solar cells with highly-conductive, low-temperature, perovskite-compatible carbon electrode. *Carbon* **2018**, *129*, 830–836. [[CrossRef](#)]
23. Lin, S.; Yang, B.; Qiu, X.; Yan, J.; Shi, J.; Yuan, Y.; Tan, W.; Liu, X.; Huang, H.; Gao, Y.; et al. Efficient and stable planar hole-transport-material-free perovskite solar cells using low temperature processed SnO₂ as electron transport material. *Org. Electron.* **2018**, *53*, 235–241. [[CrossRef](#)]
24. Vesce, L.; Stefanelli, M.; Herterich, J.P.; Castriotta, L.A.; Kohlstädt, M.; Würfel, U.; Di Carlo, A. Ambient Air Blade-Coating Fabrication of Stable Triple-Cation Perovskite Solar Modules by Green Solvent Quenching. *Sol. RRL* **2021**, *5*, 2100073. [[CrossRef](#)]

25. Chen, B.; Yang, M.; Priya, S.; Zhu, K. Origin of J-V Hysteresis in Perovskite Solar Cells. *J. Phys. Chem. Lett.* **2016**, *7*, 905–917. [[CrossRef](#)]
26. Ren, J.; Kan, Z. *Chapter 1: Origin of Hysteresis in Perovskite Solar Cells*; AIP Publishing LLC: Melville, NY, USA, 2020; Volume 1, ISBN 9780735422414.
27. Vesce, L.; Guidobaldi, A.; Mariani, P.; Di Carlo, A.; Parisi, M.L.; Maranghi, S.; Basosi, R. Scaling-up of Dye Sensitized Solar Modules. In *World Scientific Reference of Hybrid Materials*; World Scientific: Singapore, 2019; Volume 2, pp. 423–485.

Disclaimer/Publisher's Note: The statements, opinions and data contained in all publications are solely those of the individual author(s) and contributor(s) and not of MDPI and/or the editor(s). MDPI and/or the editor(s) disclaim responsibility for any injury to people or property resulting from any ideas, methods, instructions or products referred to in the content.